Design Guide: TIDA-011013

3-Phase PCB Rogowski Coil-Based Electricity Meter Reference Design

Description

This reference design aims to allow users to use different types and sizes of Rogowski coils in an electricity metering environment. The design supports a wide current range (0.25A to 115A) and 0.2% accuracy according to IEC and ANSI standards with software and hardware integration methods. This design offers a high level of flexibility and customization using a standalone analog-to-digital converter (ADC) and programmable microcontroller.

Resources

TIDA-011013	Design Folder
ADS131M08	Product Folder
MSPM0G1506	Product Folder
TLV4387	Product Folder
PCB Rogowski Coil design tool	Tool Folder

Features

- Single-chip amplifier-integrator conditioning circuit for 3-phase electricity meter
- Hardware and software integration methods
- Wide current range made for multiple metering applications
  - Residential, commercial, and industrial

Applications

- Electricity meter
- AC charging (pile) station
- AFCI circuit breaker

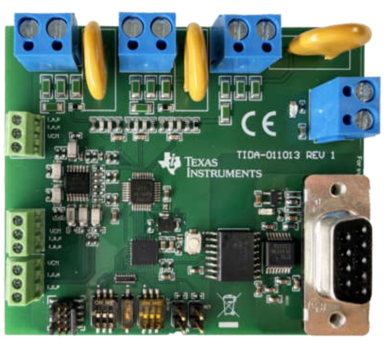

Top of Board

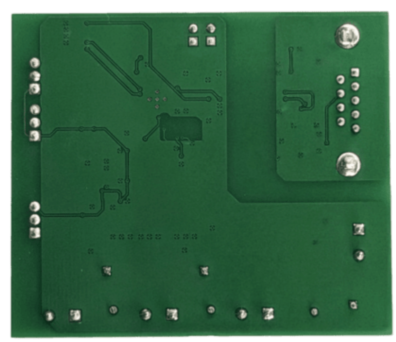

Bottom of Board

1 System Description

Electricity meter systems consist of multiple parts such as sensors, ADC, MCU, power supply, and communication. The three main components of an electricity meter are current sensing, data acquisition, and metrology engine. This design guide provides a better understanding of the main parts of an electricity meter, how to put them together, and how to evaluate and use the reference design.

1.1 Terminology

Sensitivity input to output ratio

EMF Electromotive force

ADC Analog Digital converter

MCU Microcontroller Unit

Artificial loads non-resistive loads

CMRR Common mode rejection ratio

1.2 Key System Specifications

Table 1-1. Reference Design Key Details

ITEM	DESCRIPTION
Coil sensitivity	16μV/A to 45μV/A
Coil bandwidth	10Hz to 40MHz (focus on 50Hz to 60Hz)
Amplifier gain	39V/V
Integrator bandwidth	30Hz to 6KHz
Software gain settings	1, 2, 4, 8, 16, 32, 64, 128
Number of phases	3-phases
Measured current (AC)	0.25A to 115A
Accuracy class	< 0.2%
Power requirements	3.3V external supply, j-tag

2 System Overview

Rogowski coil current sensing depends on two main concepts – Faraday's law of induction and Biot-Savart's law. A current carrying wire creates a magnetic field around it at any point in space. Assuming the current is alternating, the changing magnetic field – created by the flow of current in a wire – inside a closed loop induces an electromotive force (EMF). The output signal of a Rogowski coil is a voltage proportional to the time derivative of the primary current (di/dt) rather than the current. The absence of a magnetic core makes Rogowski coils an excellent option where magnetic saturation is an issue, such as in electricity metering.

Since the output of Rogowski coils is a voltage proportional to the rate of change in current, the output voltage is 90 degrees out of phase with the primary current. Thus, integration is needed. This reference design uses a single chip quad amplifier to amplify and integrate all three phases in one stage. In the same amplifier chip, one circuit is used to DC level-shift all the inputs to mid-voltage, eliminating the need for a negative power supply, thus driving the overall cost down.

The conditioned signal goes to a 24-bit delta-sigma simultaneous sampling ADC. The ADC converts the analog signal to a digital signal; then the data is transferred to an MCU through SPI, where the energy metrology calculation lives. Voltage, current, and phase are measured; then active and reactive power are calculated and communicated through an RS-232 cable to a PC GUI.

2.1 Block Diagram

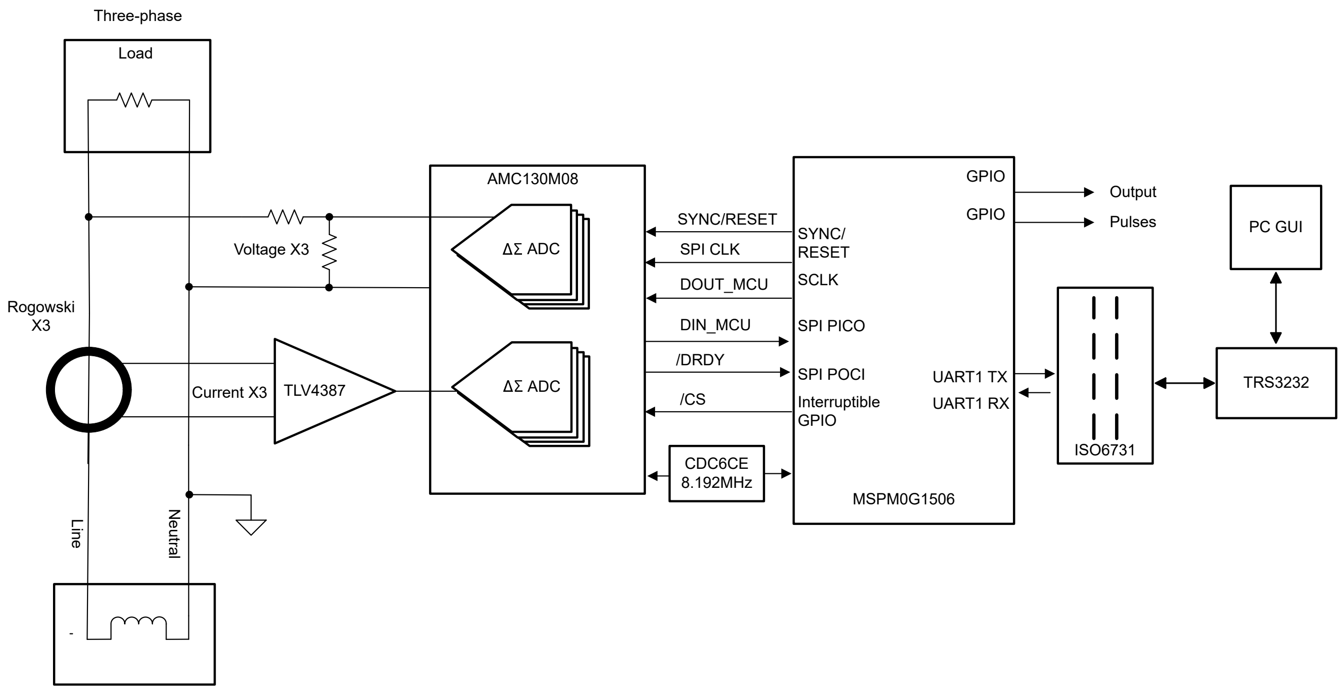

Figure 2-1. TIDA-011013 Block Diagram

2.2 Design Considerations

Using Rogowski coils for current sensing in an electricity meter poses design challenges that need to be carefully addressed. This design guide talks about challenges, design considerations, and how to properly address these challenges.

2.2.1 Low Signal Amplitude

Issue: The output voltage of the Rogowski is derived from faradays law, magnetic flux, Biot-savart, and complex analysis of the area of the coil

$$V_{out} = \frac{N\mu_0 h}{2\pi} \cdot wI_0\cos(wt) . \ln\left(\frac{b}{a}\right) \tag{1}$$

Where:

N = number of turns

μ_0 = permeability of free space

h = height of the PCB

w = angular frequency

b = outer radius

a = inner radius

t = time

Cause: The ratio of primary current to output voltage is referred to as sensitivity, typically measured in µV/A. A PCB Rogowski coil has inherently low sensitivity due to physical constraints: the PCB thickness is typically only 1.5mm, and the number of turns is limited – both of which are key factors in determining coil sensitivity.

Workaround: need to add gain to the signal. The amplifier in this reference design adds 38.9V/V to the signal and 8V/V is selected on the ADC PGA. With this combination, the meter is able to capture signals lower than 1A – considering a small Rogowski with 16µV/A sensitivity – with 0.1% accuracy.

2.2.2 Sensitivity to Noise

Issue: When high-frequency noise couples into the wire, the Rogowski coil amplifies the noise, potentially driving the output to the rails of the amplifier and ADC, leading to inaccurate measurements. In a noisy environment, the amplitude of the output is influenced by the frequency than the actual amplitude of the primary current.

Cause: The output voltage of Rogowski coils is directly proportional to the rate of change of current over time (di/dt). As frequency increases, di/dt becomes larger, which increases sensitivity. Sensitivity of a Rogowski coil increases at a rate of 20dB per decade of frequency.

Workaround: To compensate for this behavior, an integrator must be designed with a frequency response opposite that of the Rogowski coil (−20dB/dec). Since the Rogowski coil's output increases with frequency – independent of the actual current amplitude – designing an integrator with a −20dB/dec response cancels this effect. The combined frequency response becomes flat across the bandwidth, maintaining that the output is dependent on the actual current amplitude rather than frequency.

2.2.3 Integrator limitation

Issue: in electricity metering (50Hz to 60Hz), integration at low frequencies requires accumulating a signal over a large span, making it sensitive to instabilities, signal changes, and low-frequency noise. Additionally, an integrator gain approaches infinity as frequency approaches zero (DC), any low-frequency noise that couples into the signal chain is amplified and causes instability.

Cause:

Hardware integration complexity: Implementing a hardware integrator at low frequencies is very challenging due to component requirements Component size: low frequency requires large component values $\tan^{-1}(\mathrm{wRC}) = 90$, $\mathrm{z} = \frac{1}{\mathrm{jwc}}$. To get C and R must be really big value MΩ and µF.

Workaround: To get best integration, C0G/NP0 capacitors, matched resistors with low tolerance, and a low noise zero drift amplifier must be used.

2.2.4 Effect of Artificial Loads

Issue: In real-world metering scenarios, where appliances and household devices are actively consuming power, the current waveform is rarely a clean sinusoid. Different loads introduce distortion and superimpose high-frequency components onto the waveform.

Cause: Loads such as induction stoves, washers, dryers, fans, and lighting which exhibit conducted electromagnetic interference characteristics and transient bursts

Workaround: need an integrator that filters the high voltage spikes and the effect of non-resistive loads before amplifying the signal.

2.2.5 Stray Magnetic Field Interference

Issue: Since Rogowski is a di/dt current sensor, it detects the change in flux over time. If there is a stray magnetic field close to the meter, the meter will pick up the magnetic fields and cause inaccurate billing.

Cause: Rogowski coils are sensitive to stray magnetic fields primarily because they are air-core sensors that rely on detecting the magnetic flux derivative, lacking a high-permeability shielding core to reject external fields.

Workaround: To address this, a differential coil with interleaved return loops is required. When exposed to external magnetic fields, this configuration generates a common-mode signal, which is then canceled by the differential amplifier. This reference design covers the differential amplifier implementation in detail.

2.2.6 Crosstalk

Issue: Crosstalk occurs when sensing coils are placed close to a current-carrying wire, or when Rogowski coils are used in a 3-phase system. This interference leads to inaccurate current measurements due to the influence of external magnetic fields generated by neighboring phases.

Cause: The Biot-Savart Law describes the magnetic field produced by a straight current-carrying wire at any point away from the center of the wire

$$B_1 = \frac{\mu_0 I_1 \sin(wt)}{2\pi r_1} \tag{2}$$

Where B_1 is the magnetic field generated by wire 1 at any point distance (r_1) from the center of the wire.

$$B_2 = \frac{\mu_0 I_2 \sin(wt)}{2\pi r_2} \tag{3}$$

Where B_2 is the magnetic field generated by wire 2 at any point distance (r_2) from the center of the wire.

The sum of magnetic fields at any point between the wires is as below:

$$\sum B = B_1(r_1) + B_2(r_2)\cos(\theta) \tag{4}$$

Where (θ) is the orientation between B_1 and B_2 and (θ) can only be 180 or 0 if the two wires are parallel to one another.

- – If (θ) = 180°, the currents flow in the same direction and the magnetic fields oppose each other. The sum of magnetic fields increases as distance is closer to either wire and cancel at midpoint between the two wires if currents are the same.
  - If (θ) = 0°, the currents flow in opposite directions and the magnetic fields are in the same direction reinforcing one another, producing a uniform net field between the wires. The overall field magnitude increases as the spacing between the wires decreases and decreases as the spacing increases.
  - These are the two worst cases and non-realistic. Crosstalk effect can be at any point between the two worst cases.

Workaround:

1. To address this, a differential coil with interleaved return loops is required. When exposed to external magnetic fields, this configuration generates a common-mode signal, which is then canceled by the differential amplifier. This reference design covers the differential amplifier implementation in detail.
2. Software calibration and crosstalk compensation.

2.2.7 Mechanical Limitations

Issue:

- Coil geometry: Non-circular coil geometries are often required to efficiently fit around busbars without wasting space.

- Remote placement: Some applications require the sensing element to be located away from the metrology or signal-conditioning circuitry.
- Retrofit inconvenience: In scenarios where a wire or a harness is already installed, fitting a PCB Rogowski coil can be disruptive and impractical.

Causes:

- PCB Rogowski coils are inherently susceptible to noise pickup along the connection to the metrology board. This noise can degrade measurement accuracy.
- Rigid, fixed coil geometries make fitting difficult, as they require physical modification or interruption of an existing installation to wrap around a conductor or busbar.

Workarounds:

1. A flexible or openable coil design that can simply be wrapped around a conductor or busbar offers a more practical and less intrusive alternative.
2. Signal conditioning placement close to sensing coil.

2.2.8 Human Errors

Issues:

- Output voltage optimization: Maximizing output voltage requires increasing the effective surface area by adding more turns to the coil. However, scaling the number of turns while maintaining performance is not straightforward when done manually.
- Loop symmetry: Maintaining strict symmetry in the sensing loops is one of the most difficult aspects of PCB Rogowski coil design. Even small geometric mismatches can introduce imbalance, leading to waveform distortion and increased susceptibility to external magnetic field coupling.
- Closed-loop integrity: Maintaining that all coil turns remain symmetric and form a properly closed loop is critical to preserving the intended differential architecture. Achieving this level of precision by hand – especially in complex or non-standard geometries – is highly challenging and error-prone.

Cause: Rogowski coil is fundamentally constructed by winding a wire around a non-magnetic core, with one end routed back through the center to create a return path. The entire assembly is then shaped into a closed loop, resulting in two distinct loop types within the design:

1. Sensing loops
2. Return loops

Since output voltage is directly dependent on the number of turns and the coil geometry, any asymmetry or inconsistency introduced during manual construction directly impacts measurement accuracy and noise immunity.

Workaround: Automating coil design process through the PCB Rogowski coil design tool.

2.3 Highlighted Products

2.3.1 TLV4387

TLV4387 is a precision amplifier offering state-of-the-art performance. With zero-drift technology, the TLVx387 offset voltage and offset drift provide unparalleled long-term stability. With a mere 570μA of quiescent current, the TLVx387 can achieve 5.7MHz of bandwidth, a broadband noise of 8.5nV/√Hz, and a 1/f noise at 177nVPP. These specifications are crucial to achieve extremely high precision and no degradation of linearity in 16-bit to 24-bit analog to digital converters (ADCs). TLV4387 feature flat bias current over temperature; therefore, little to no calibration is needed in high input impedance applications over temperature.

2.3.2 ADS131M08

The ADS131M08 is an eight-channel, simultaneously sampling, 24-bit, delta-sigma (ΔΣ), analog-to-digital converter (ADC) that offers wide dynamic range, low power, and energy-measurement-specific features, making the device an excellent fit for energy metering, power metrology, and circuit breaker applications. The ADC inputs can be directly interfaced to a resistor divider network or a power transformer to measure voltage or to a current transformer or a Rogowski coil to measure current. The individual ADC channels can be independently configured depending on the sensor input. A low noise, programmable gain amplifier (PGA) provides gains ranging from 1 to 128 to amplify low-level signals. Additionally, this device integrates channel-to-channel phase calibration and offset and gain calibration registers to help remove signal-chain errors. A low-drift, 1.2V reference is integrated into the device reducing printed circuit board (PCB) area. Optional cyclic redundancy checks (CRCs) on the data input, data output, and register map maintain communication integrity.

2.3.3 MSPM0G1506

The TI MSPM0G1506 is a low-power MCU consisting of devices with varying degrees of analog and digital integration that allow customers to find the MCU that meets project needs. MSPM0G1506 includes Arm Cortex-M0+ platform with a holistic ultra-low-power system architecture, allowing system designers to increase performance while reducing energy consumption.

2.3.4 ISO6731

The ISO6761 device is high-performance, six channel digital isolators good for cost-sensitive applications requiring up to 5000 VRMS isolation ratings per UL 1577. These devices are also certified by VDE, TUV, CSA, and CQC. The ISO676x devices provide high electromagnetic immunity and low emissions at low power consumption, while isolating CMOS or LVCMOS digital I/Os. Each isolation channel has a logic input and output buffer separated by TI's double capacitive silicon dioxide (SiO2) insulation barrier.

2.3.5 TPS70933

The TPS709 series of linear regulators are ultra-low, quiescent current devices designed for power sensitive applications.

2.3.6 TRS3232

The TRS3232 consists of two line drivers, two line receivers, and a dual charge-pump circuit with ±15kV ESD protection terminal-to-terminal (serial port connection terminals, including GND). The device meets the requirements of TIA/EIA-232-F and provides the electrical interface between an asynchronous communication controller and the serial-port connector. The charge pump and four small external capacitors allow operation from one 3V to 5.5V supply. The devices operate at data signaling rates up to 250kbps and a maximum of 30V/µs driver-output slew rate.

2.3.7 CDC6CE

The CDC6Cx device is a low jitter, low power, fixed-frequency oscillator which incorporates the BAW as the resonator source. The device is factory programmed by specific frequency and function pin. With a frequency control logic and output frequency divider, the CDC6CE can produce any frequency within the specified range providing a single device family for all frequency needs. The high-performance clocking, mechanical stability, lower power consumption, flexibility, and small package options for this device are designed for reference clock and core clocks in Industrial, Telecom, Data and Enterprise Network and Personal Electronics end equipment.

3 System Design Theory

This reference design employees the use of TI's newest PCB Rogowski design tool. The new design tool addresses PCB coil geometries challenges such as asymmetries with trace placements, loop mismatches, and human errors with manual coil design. TI devices solve Rogowski design challenges of integration, low sensitivity of the coil, crosstalk, effect of external magnetic fields, and sensitivity to noise.

3.1 Rogowski Coil

The coil functions as a differential coil with matching return loops. Distance from the conductor determines Rogowski sensitivity by controlling magnetic field density and loop area. External magnetic fields couple into the signal when loop path mismatch occurs in this differential signal with high gain. The coil design uses a novel layout to match loop paths while offsetting inner vias. This allows greater loop density. Four interleaved Rogowski coils accomplish this design. Two coils, an outer and inner coil, wind in opposite directions and connect in series. These connect differentially with the other pair wound identically. This topology provides inductive and capacitive noise rejection while increasing coil density. The Rogowski design tool provides PCB coils with a center tap so that the signal can be biased to a common-mode voltage, eliminating the need for a negative supply and driving the overall cost down.

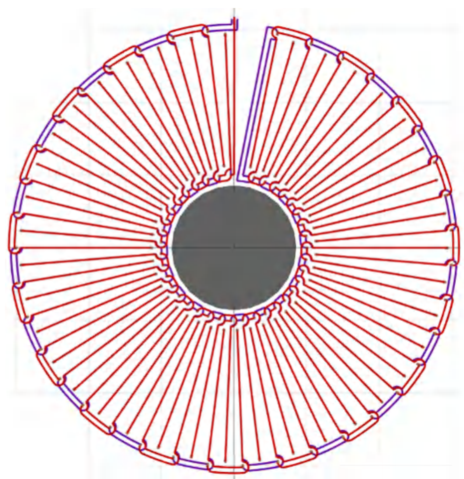

Figure 3-1. Rogowski Coil Winding Layout

3.2 Hardware Integrator

An integrator provides a flat response across the full PCB Rogowski bandwidth as well as amplifying the low amplitude low frequency signal without accumulating error over time since an integrator has infinite gain at DC.

A differential integrator circuit was designed to address PCB Rogowski design challenges and achieve class 0.2 accuracy according to ANSI and IEC standards across a wide current range.

TLV4387 was chosen for this application because it is an excellent low noise zero-drift amplifier that also has high CMRR to reject common mode generated by external magnetic fields.

Three circuits in TLV4387 are used to condition each Rogowski output signal in a 3-phase system and the fourth one is used to generate a common-mode voltage. ADC input is driven pseudo-differentially so that noise from common-mode bias is removed.

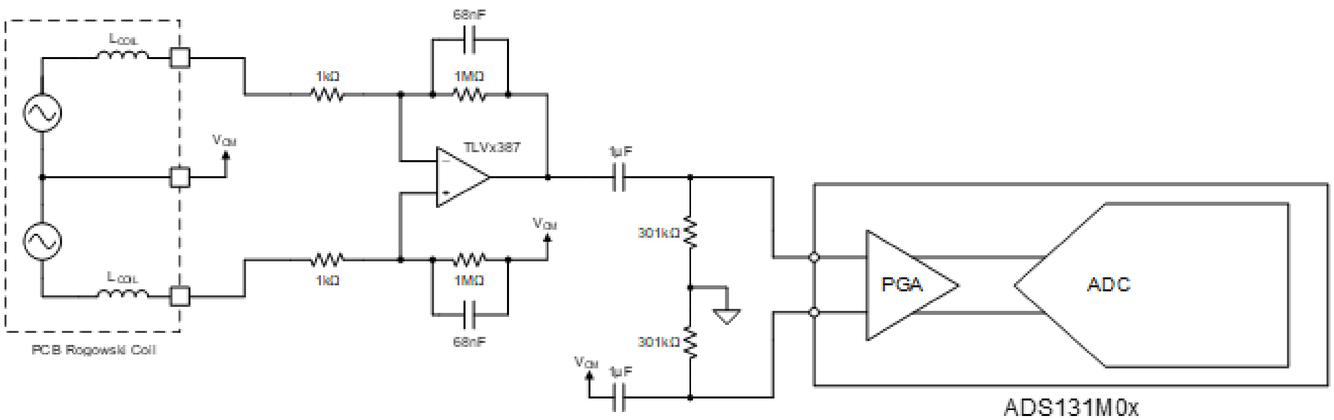

Figure 3-2. Differential Integrator-Amplifier Circuit

4 Hardware, Software, Testing Requirements, and Test Results

4.1 Hardware Requirements

The following hardware components and specifications are required for proper system operation and performance of the reference design:

1. 3.3VDC external supply
2. RS-232 cable
3. High-voltage safety box
4. Flat head screwdriver
5. 3× 1AWG wires for current
6. 4× 14AWG to 10AWG wires for voltage
7. Accurate AC power supply
8. AC load
9. 3× twisted triplet (coil to board connection)

4.2 Software

The following software components and specifications are required for proper system operation and performance of the reference design:

1. RS-232 to USB driver
2. Metrology GUI
3. MSPM0SDK

Note: metrology code is already flashed onto reference design.

4.3 Test Setup

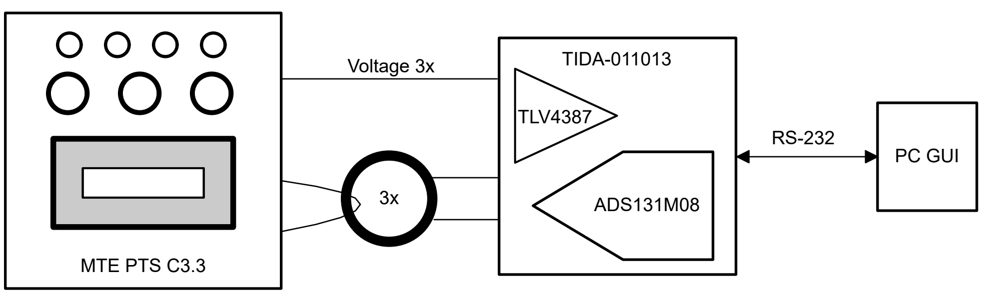

Figure 4-1. Test Setup Block Diagram

4.3.1 Header Information

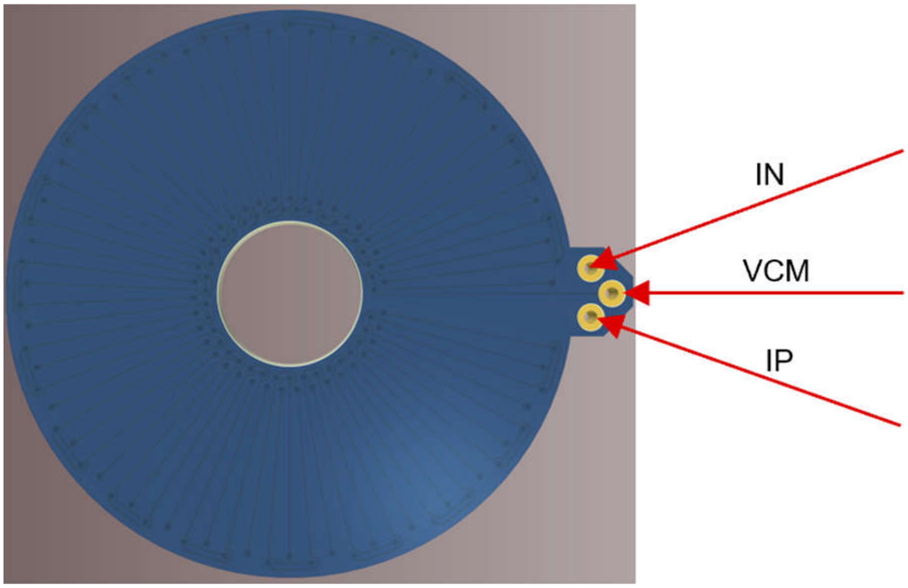

Figure 4-2. Rogowski Coil Connection Guide

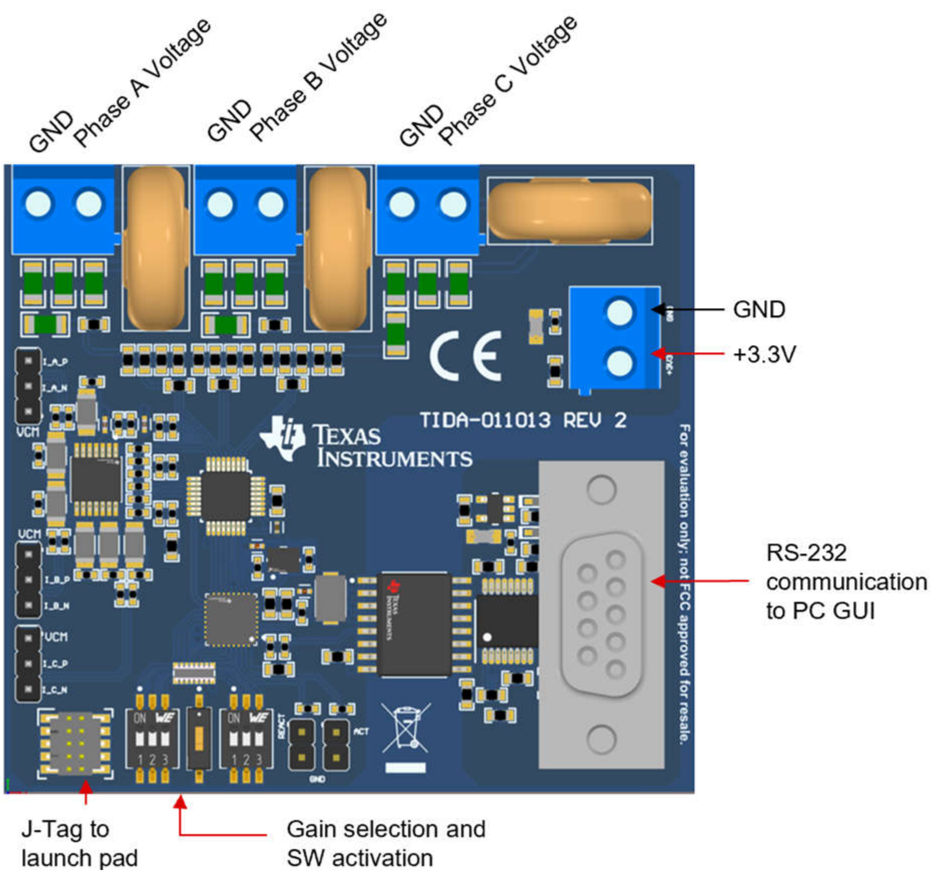

Figure 4-3. TIDA-011013 Connection Guide

4.4 Getting Started

4.4.1 Software Installation

Two pieces of software must be installed on the PC being used to evaluate the reference design. The first piece is the drivers for RS-232 cable must be installed from the manufacturer's website. The second piece of software needed is the MSPM0-SDK. The SDK package includes the Energy Metrology GUI.

4.4.2 GUI Setup

Before running the GUI, plug the USB to RS-232 cable into the PC and verify the COM port used. On a Microsoft Windows PC, open the Device Manager and scroll down to Ports (COM and LPT). Find the Prolific USB Serial COM Port and note the port used.

Open the folder on the PC that contains the metrology GUI. By default, the GUI is in C:\ti\mspm0_sdk_(version)\tools\metrology_gui. Before running the calibrator.exe file, open and edit the calibration-config.xml file. Open the calibration-config.XML file with a text editor and search for. The line following the meter position must use the same COM port that is associated with the PL2303GS COM port. Be sure to save any changes before running the calibrator.exe file.

Once GUI setup is done, open calibrator.exe.

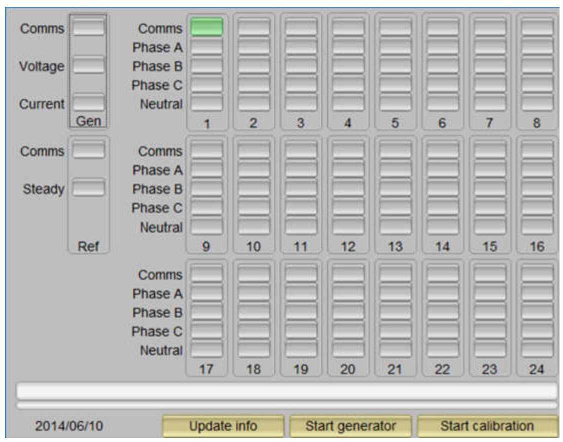

Figure 4-4. GUI Startup Page

Once clicking on calibrator.exe, the GUI startup page appears, and click the green button to access meter readings and calibration. If the button is red, that means that the connection between TIDA-011013 and PC GUI has not been established. To debug connection, make sure that the COM port (whatever shown in device manager) and Baude rate (9600) are set to the correct configurations then try reconnecting.

Once connected click on the green button to access meter readings and calibration.

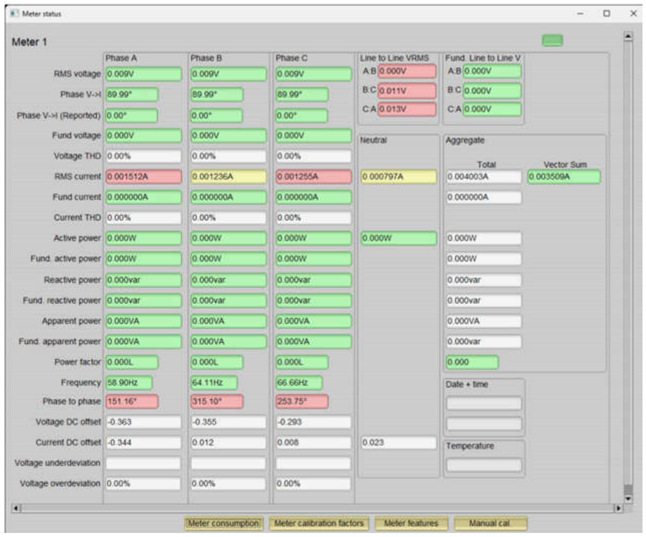

Figure 4-5. Meter Readings and Calibration

4.4.2.1 Calibration

Once GUI is opened and updating, meter is ready for calibration

---

Note

Before calibration, make sure PGA gain is set to 8 (for max current 120 and coil sensitivity is 25µV/A and lower) using DIP switches on board. Adjust gain according to max current. Every time gain is changed, the reset button must be clicked to reset settings.

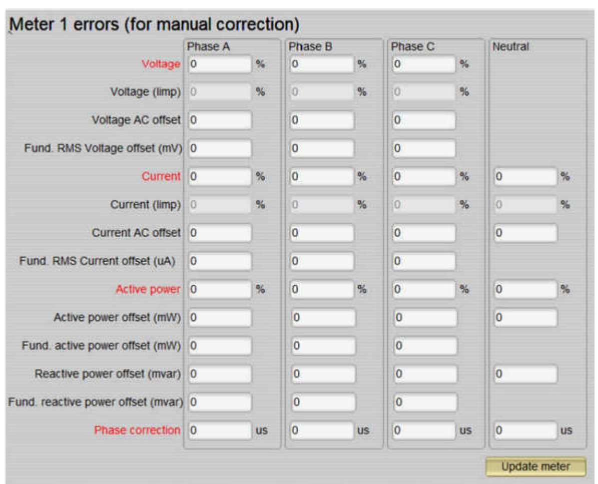

Figure 4-6. Manual Calibration Page

Calibration is recommended to be done at nominal values:

- 120Vrms
- 15 Arms
- 50Hz – 60Hz
- 60° phase offset

Input nominal values to the meter. Open manual calibration tab in the GUI shown in figure 4-6. Calibrate phase first by adding or subtracting microseconds to the phase correction cell for each phase.

$$\frac{60 - (\text{measuredphaseoffset})}{360} \tag{5}$$

Once phase is calibrated, change phase V->I to 0° and calibrate voltage, current, and active power. Error correction factors are calculated using this equation:

$$\left(\left(\frac{\text{measuredvalue}}{\text{sourcevalue}}\right) - 1\right) \cdot 100 \quad (6)$$

Copy correction factors into the manual calibration tab (red Cells) for each phase and click update meter. Now meter is calibrated and ready for evaluation and testing.

4.5 Test Results

- PCB Rogowski coil that was used for testing was made by the Rogowski design tool with sensitivity of 20µV/A.
- TIDA-011013 targets 0.1 – 0.2 class accuracy for class 100 meters (1A min current and 100 max current).
- Accuracy measurements were taken at currents from 0.25A up to 115A

4.5.1 Active Power Accuracy Measurements

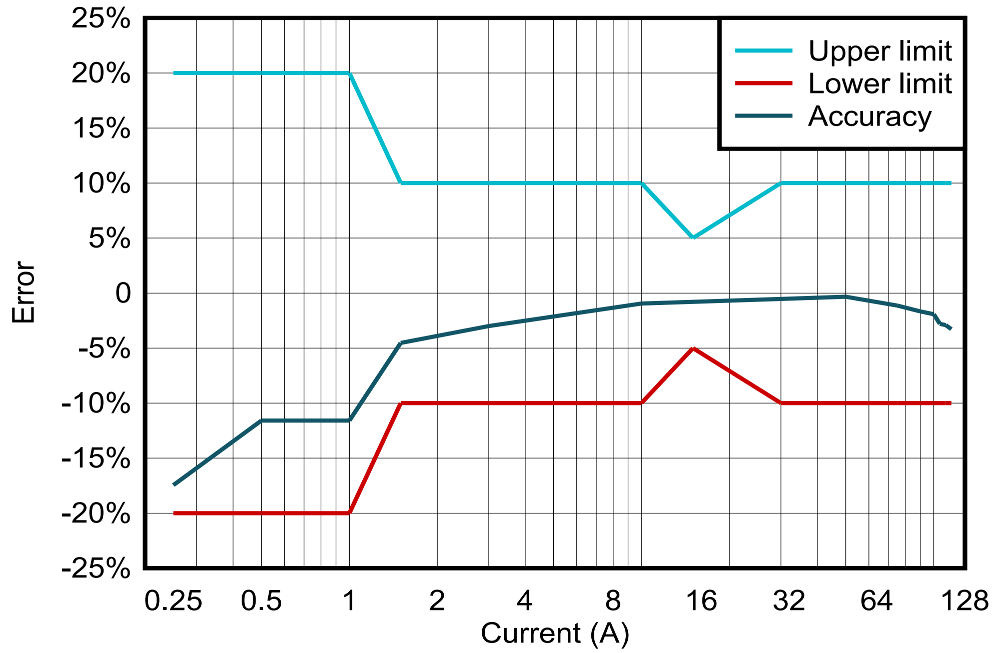

Figure 4-7. Active Power Accuracy Measurements at Full Current Range PF=1

Observations: TIDA-011013 was able to achieve 0.1 class accuracy at and outside full current range.

4.5.2 Active Power Accuracy Measurements (PF≠1)

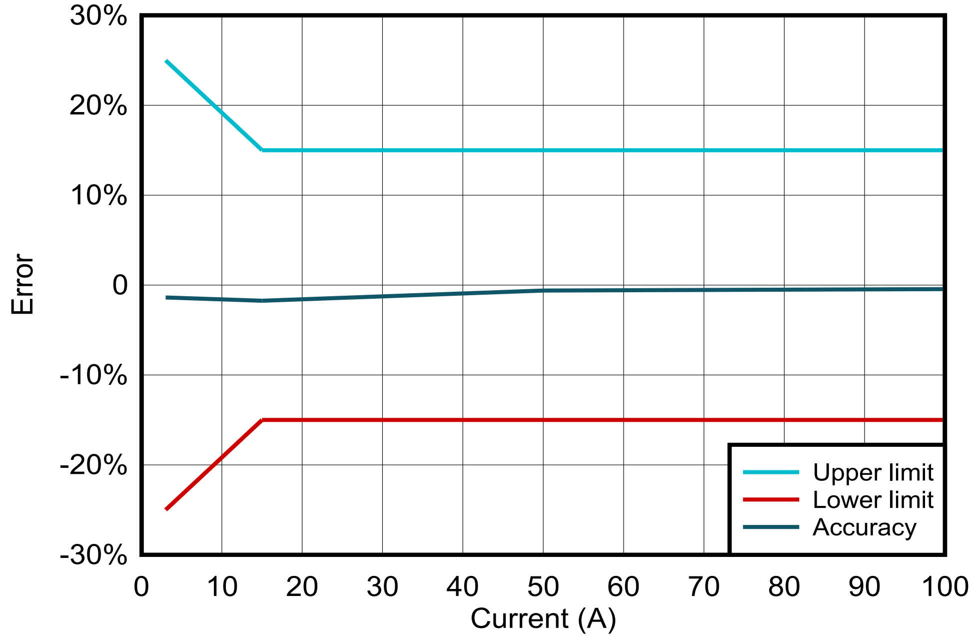

Figure 4-8. Active Power Accuracy Measurements at Full Current Range PF=0.5 (Leading)

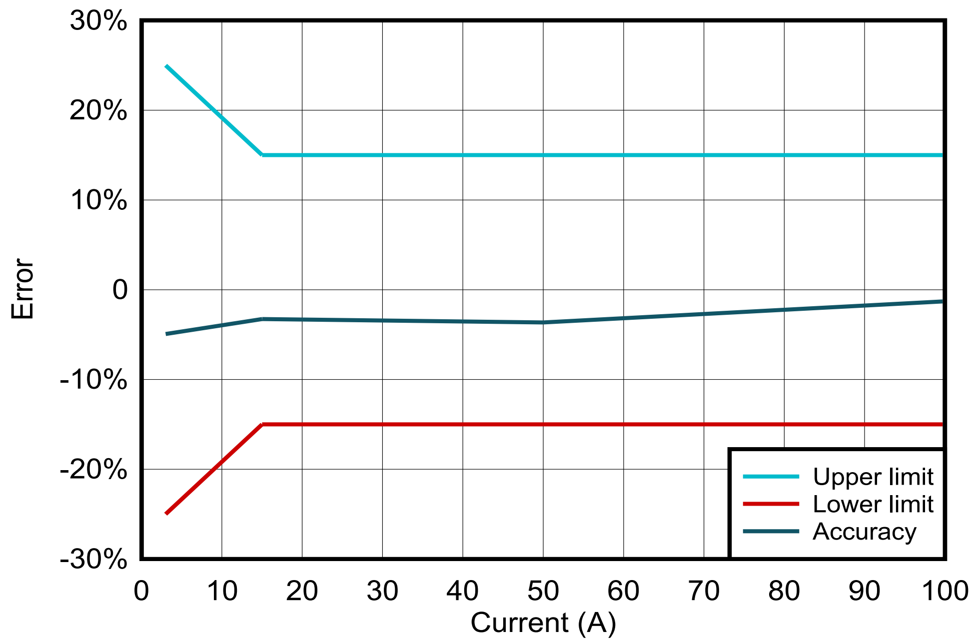

Figure 4-9. Active Power Accuracy Measurements at Full Current Range PF=0.5 (Lagging)

Observations: TIDA-011013 was able to achieve 0.1 class accuracy at full current range.

4.5.3 Reactive Power Accuracy Measurements

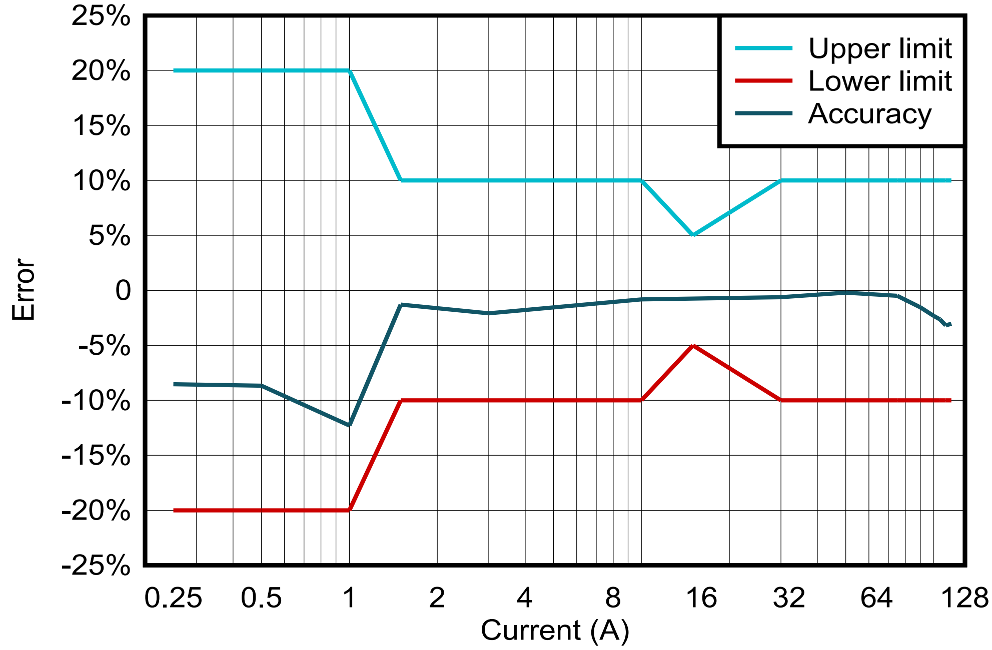

Figure 4-10. Reactive Power Accuracy Measurements at Full Current Range PF=1

Observations: TIDA-011013 was able to achieve 0.1 class accuracy at and outside full current range.

4.5.4 Reactive Power Accuracy Measurements (PF≠1)

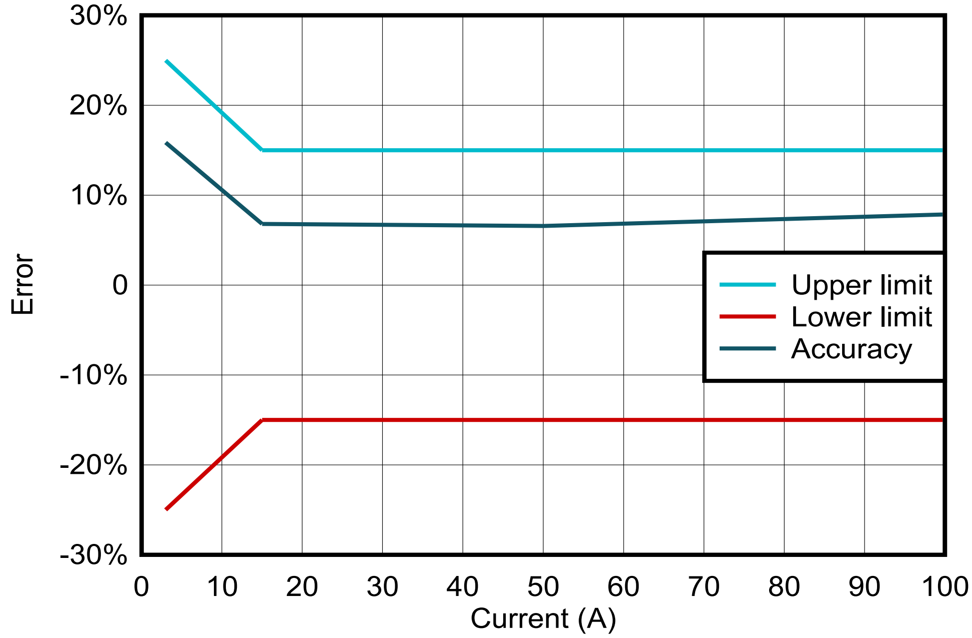

Figure 4-11. Active Power Accuracy Measurements at Full Current Range PF=0.5 (Leading)

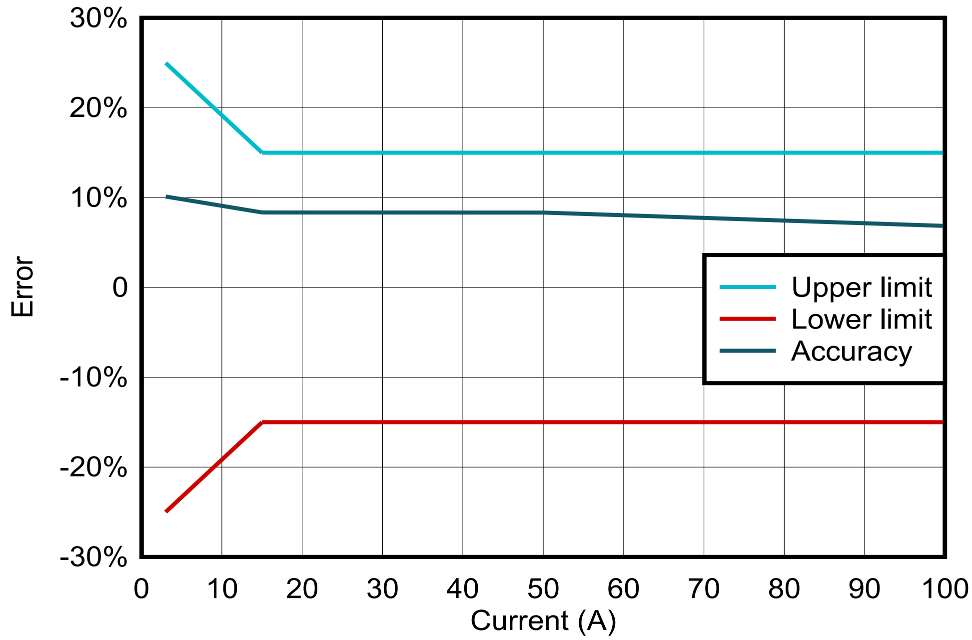

Figure 4-12. Active Power Accuracy Measurements at Full Current Range PF=0.5 (Lagging)

Observations: TIDA-011013 was able to achieve 0.1 class accuracy at full current range.

4.5.5 Voltage Variation Accuracy Measurements

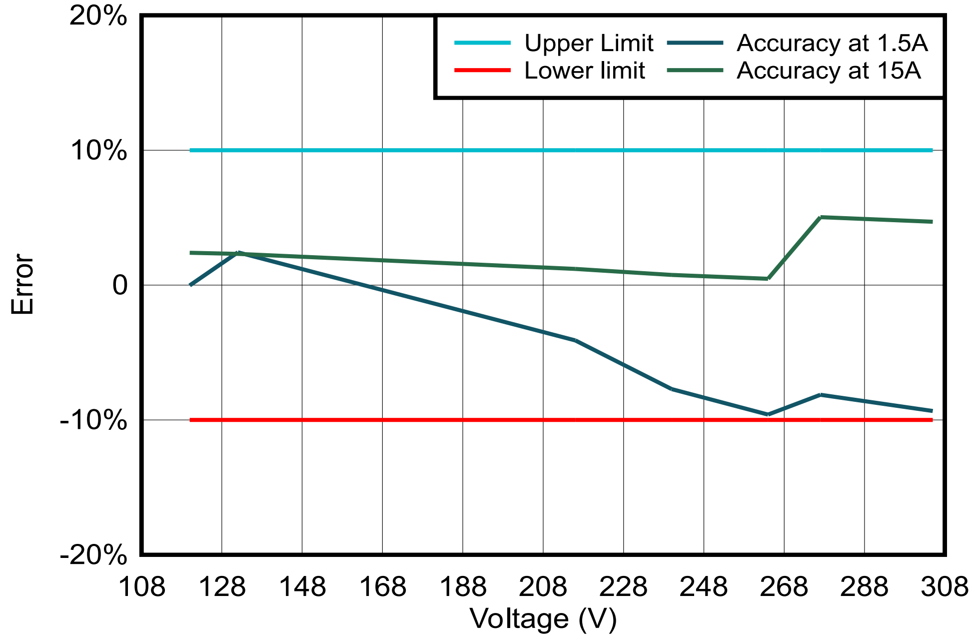

Figure 4-13. Variation of Voltage Accuracy Measurements at Different Current Levels

4.5.6 Frequency Variation Accuracy Measurements

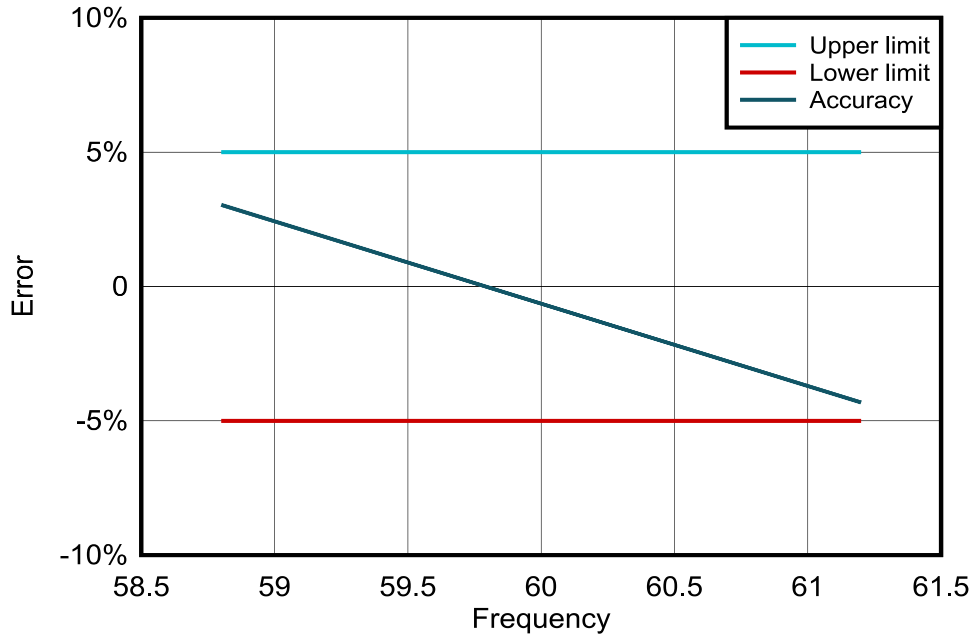

Figure 4-14. Variation of Frequency Accuracy Measurements at ±2% of Reference Frequency

Observations: TIDA-011013 was able to achieve 0.1 class accuracy at full frequency range.

4.5.7 Equality of Current Circuits Accuracy Measurements

Objective: test the accuracy of reference design when all three phases are connected (reference), unplug all phases except one, and record accuracy measurements only when one phase is connected at a time.

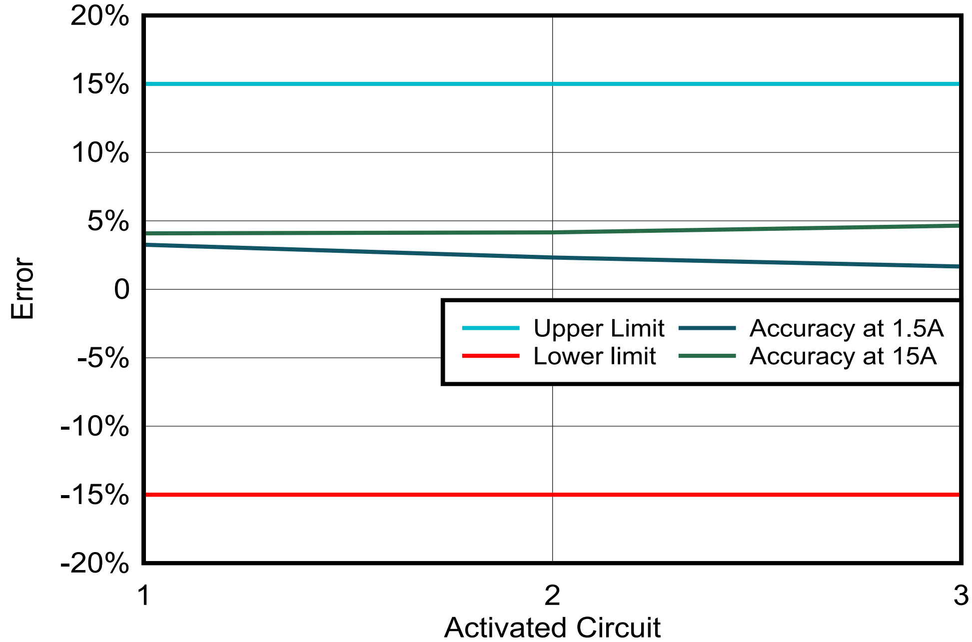

Figure 4-15. Equality of Current Circuits Accuracy Measurements

Observations: TIDA-011013 was able to achieve 0.1 class accuracy when only one circuit is activated at a time at different current levels.

4.5.8 Phase Reversal Accuracy Measurements

Objective: test the accuracy of reference design when all three phases are connected (reference), reverse the order of phases (ABC to CBA), Record the accuracy after reversing the order, and compare accuracies. Deviation in accuracy must not exceed 0.1 class accuracy limits.

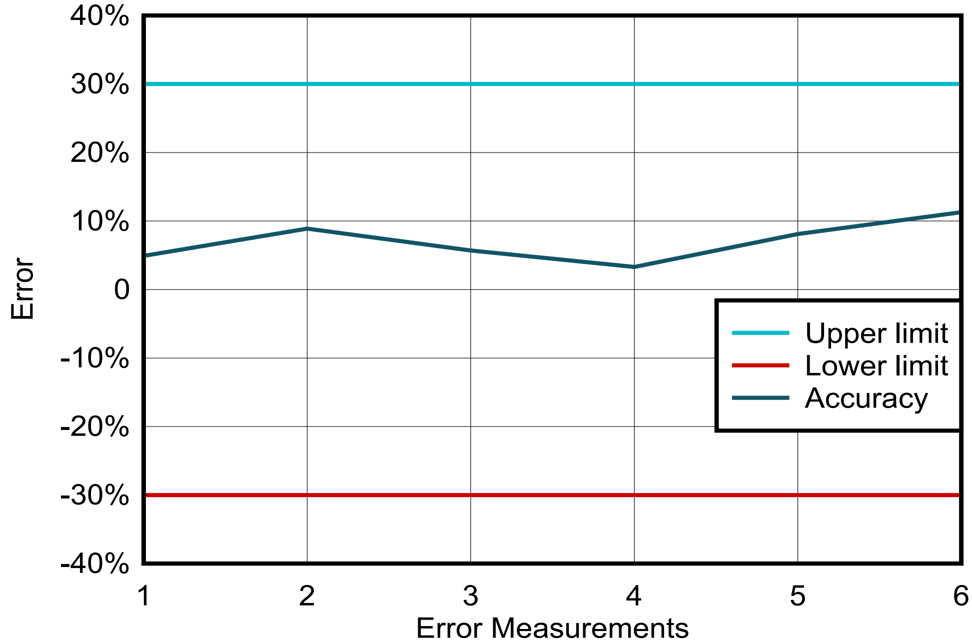

Figure 4-16. Equality of Current Circuits Accuracy Measurements

Observations: six different accuracy readings were taken over the span of 30 minutes (five minutes between each error reading). TIDA-011013 was able to achieve 0.1 class accuracy when the sequence of phases is reversed.

4.5.9 Temperature Variation Accuracy Measurements

Objective: record the accuracy of reference design, place reference design in a temperature-controlled chamber, change temperature to -20°C, wait for an hour, and record error measurements. Repeat the same process for temperature 50°C and record error measurements.

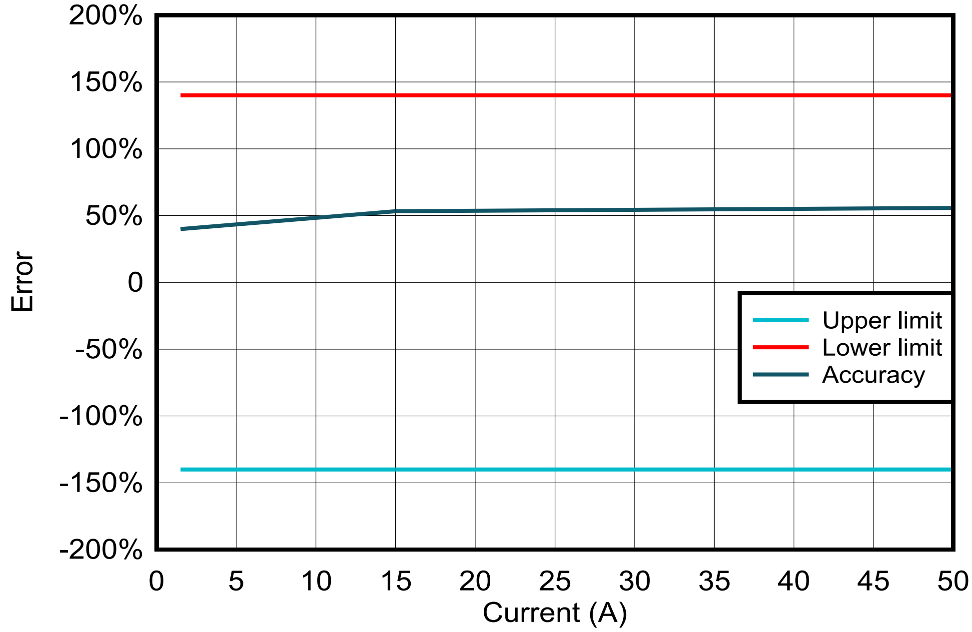

Figure 4-17. Accuracy Measurements at 50°C

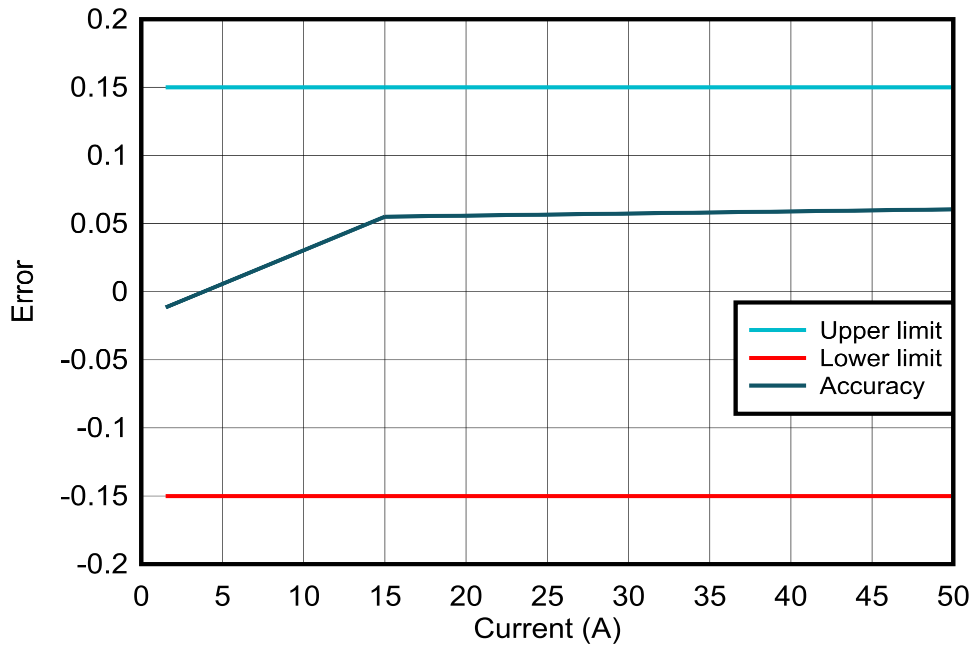

Figure 4-18. Accuracy Measurements at -20°C

Observations: TIDA-011013 was able to achieve 0.1 class accuracy at a wide temperature range.

4.5.10 Crosstalk Accuracy Measurements

Objective: calibrate each phase independently, apply 20A on phase one and record measured current on phase one, apply 100A on phase two with 180° phase offset (worst case), and observe the effect of crosstalk on phase one. Repeat process for phase two and phase three. Effect of crosstalk must stay below allowable limit.

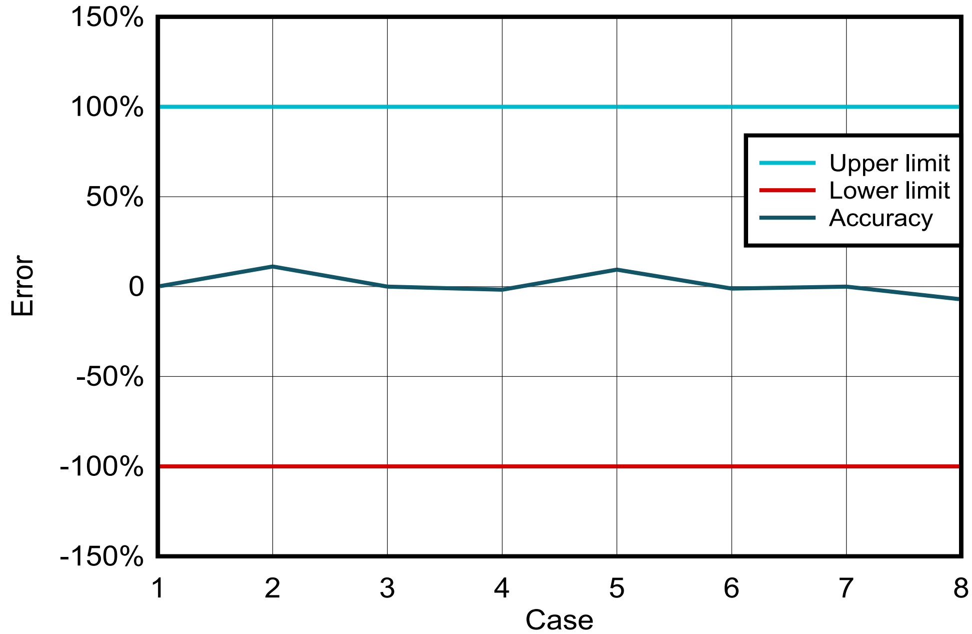

Figure 4-19. TIDA-011013 Immunity to Crosstalk

Observations: x-axis represents the different cases that TIDA-011013 was tested at. Cases are described in table below. TIDA-011013 was able to stay within the allowable error with external magnetic fields generated by neighboring phases at all cases.

Table 4-1. Crosstalk Test Cases

Case	I1	I2	I3
1	20A	0	0
2	20A	100A	0
3	0	20A	0
4	100A	20A	0
5	0	20A	100A
6	100A	20A	100A
7	0	0	20A
8	0	100A	20A

4.5.11 Effect of External Magnetic Fields Accuracy Measurements

Objective: calibrate reference design when there is no external magnetic fields in the area, place reference design inside a 1 meter diameter circular wire while pushing 60A/turn, and record effect of external magnetic fields by comparing error measurements to reference measurements.

Setup: for this test, Helmholtz coils were used to generate the external magnetic fields. See Figure 4-20.

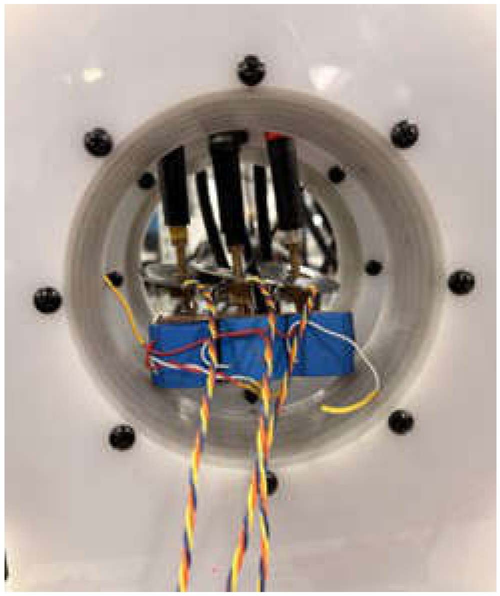

Figure 4-20. PCB Rogowski Coils Inside Helmholtz Coils

Magnetic field generated by the Helmholtz coils = 0.5mT

Results:

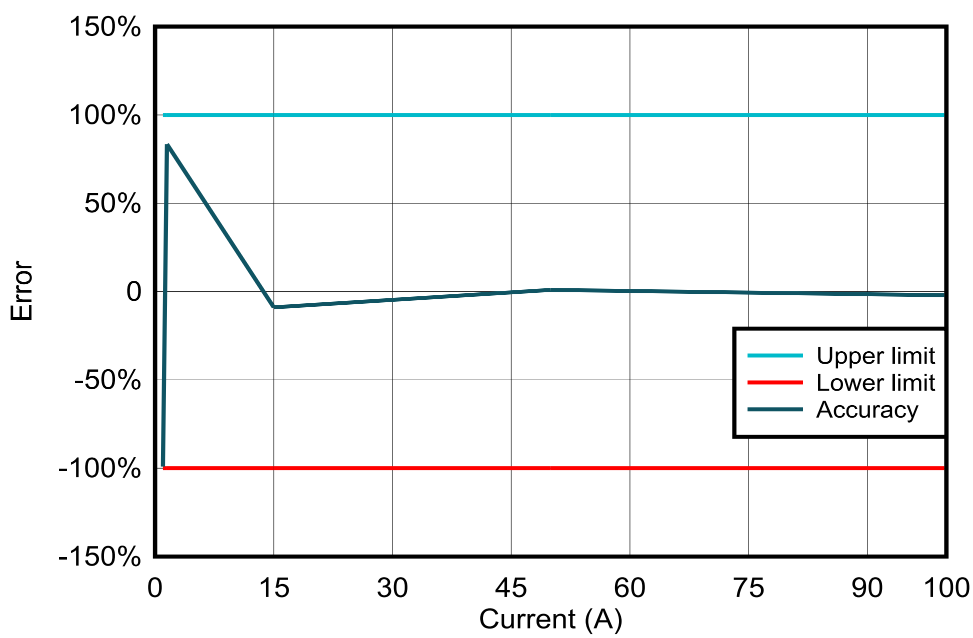

Figure 4-21. TIDA-011013 Accuracy Measurements With The Effect of External Magnetic Fields

Observations: TIDA-011013 was able to stay within the allowable error with external magnetic fields generated by Helmholtz coil.

5 Design and Documentation Support

5.1 Documentation Support

1. Texas Instruments, *LMR436x0-Q1, 36V, 1A / 2A, Automotive Buck Converter With < 2.5μA IQ at 150°C TJMAX in 4mm2 HotRod QFN* data sheet
2. Texas Instruments, *TPS62850x-Q1 2.7V to 6V, 1A, 2A, 3A, Automotive, Step-Down Converters in an SOT583 Package* data sheet
3. Texas Instruments, *TLIN1021A-Q1 Fault-Protected LIN Transceiver with Inhibit and Wake* data sheet

Trademarks

All trademarks are the property of their respective owners.

6 About the Author

DANIEL MAAYA is a systems engineer at Texas Instruments in Dallas, where he focuses on the development of precision analog front-end designs for power metering and grid infrastructure applications. Daniel brings to this role a multidisciplinary background in electrical and Power electronics with deep expertise in signal conditioning, metrology compliance (ANSI/IEC), power converters, and Rogowski coil-based sensing systems. He has hands-on experience with both analog hardware design and system-level integration, including EMC testing and calibration for high-accuracy measurement.